Proceeding of the 13th National Mechanical Engineering Conference
2-3 December 1999, Royal Cliff Beach Resort Hotel, South Pattaya, Cholburi

The Design and Development of The FMRL 60x18 cm^2 Wide-Angle Screened-Diffuser Blower Tunnel Part III: The Settling Chamber, The Contraction, and The Wind Tunnel

Tanarit Sakulyanontvittaya, Pornpong Ngow, Authapoch Prasartkarnkha, Sirichai Chalokepunrat, Alongkorn Pimpin and Asi Bunyajitradulya

Fluid Mechanics Research Laboratory, Department of Mechanical Engineering,
Faculty of Engineering, Chulalongkorn University,
Bangkok 10330, Thailand
Tel. 218-6645, 218-6647; Fax. 252-2889; E-mail basi@chula.ac.th

Abstract

This is Part III of a series of three papers describing the design and development of the Fluid Mechanics Research Laboratory (FMRL) 60x18 cm^2 wide-angle screened-diffuser blower tunnel. In this part, the design and development of the settling chamber and the contraction are described. The calibration schemes for the determination of the quality of flow at the contraction exit and the results are reported. The results show that the tunnel performs satisfactorily. For the current configuration, the maximum speed of the tunnel is 13.95 m/s with the non-uniformity of the freestream less than $\pm$ 1.5% and with the average boundary layer thickness less than 3 mm. At another lower speed, the speed of 7.29 m/s, the non-uniformity is less than $\pm$ 2.2% and the average boundary layer thickness is less than 4 mm.

1. Introduction

As discussed in Part I, generally, the desired standard condition for the flow in the test section of a wind tunnel is steady, uniform, with low freestream turbulence level. Other qualities that may be of concern are, for example, the thickness and the uniformity of the distribution of the thickness of the boundary layer and the uniformity of the skin friction coefficient at the contraction exit. Depending on the flow that is to be investigated and on the flow diagnostics that is to be employed, the requirements of these qualities vary. For example, for high quality flow visualization, very low freestream turbulence level is often required of smoke tunnels. This is also true for wind tunnels that are used for study of laminar-to-turbulent transition.

Although the exit flow from a screened diffuser of a blower tunnel can be made fairly uniform, it is often far from being uniform and steady enough. And, most importantly, it often has swirl and high freestream-turbulence level. To condition the exit flow from the diffuser, two main components are employed: a settling chamber and a contraction. In a settling chamber, there are a honeycomb and a series of screens. A honeycomb is mainly used for removing swirl and lateral mean velocity variation, while a series of screens is used for removing mean velocity variation as well as turbulence. On the other hand, a contraction is used for accelerating the flow to a desired speed in the test section as well as for removing mean velocity variation and freestream turbulence.

In this part, the settling chamber and the contraction of the FMRL wide-angle screened-diffuser blower tunnel are described. The calibration results for the tunnel, specifically the uniformity of the mean velocity and the boundary layer thickness, are reported. Unfortunately, owing to the lack of measuring instrument, the data on turbulence intensity are not available. We shall report this when they become available.

2. Settling chamber

Two main components in a settling chamber are a honeycomb and a series of screens. Honeycombs come in various cell shapes and sizes. The most common shapes commercially are probably a hexagonal, a circular, and a square. However, Bradshaw and Pankhurst (1964) suggested that in wind tunnel application the cell shape was not so critical so long as the ratio between its length and diameter was between 6 to 8. Thus, the choice depended more on the availability. On the other hand, the cell size should be less than the smallest lateral wavelength of velocity variation. Generally, 50 cells per settling chamber diameter should be adequate for a settling chamber fitted with a number of screens.

It is important to note that, although honeycombs, as well as screens, are used to suppress turbulence, they also generate turbulence. For a honeycomb, it suppresses the incoming turbulence mostly through the inhibition of lateral components of the fluctuating velocity. At the same time, it generates turbulence through shear-layer instabilities in its near wake region. Loehrke and Nagib (1976) studied these two mechanisms and found that the character of the fine shear layers emerging from a honeycomb had strong influence on the level, structure, and decay of turbulence farther downstream. By putting a fine mesh screen at various downstream distances from

the exit plane of a honeycomb, they were able to modify the characteristics of the emerging shear layers. Their results indicated that, the reduction of turbulence was effective as long as the screen was positioned upstream of the point where appreciable growth of large-scale instabilities had taken place. This corresponded to the distance of approximately 5 honeycomb meshes. In addition, their results suggested that the most effective location for the screen was right at the exit plane. As a result, for effective suppression of turbulence they recommended the use of a honeycomb in combination with a screen, the honeycomb cell length as short as possible provided that the cell length to diameter ratio was approximately equal to or more than 10, and the screen installed within 5 honeycomb meshes downstream of the exit plane of the honeycomb.

A series of screens is generally used in a settling chamber for removing mean velocity variation and turbulence from the flow downstream of a honeycomb. We have reviewed some theoretical and experimental results for flow through screens from past studies in Part II. At this point, it suffices to emphasize for reference and to add some of the relevant points for the application of screens in a settling chamber.

Firstly, for flow through a screen, the factors of reduction of mean velocity variation were given by

$$\frac{1+\alpha-\alpha K'}{1+\alpha+K'}, \quad \text{for longitudinal component,} \qquad (1)$$

and α, for lateral component, (2)

(Batchelor, 1953), and the factors of reduction of turbulence intensity were given by,

$$\frac{0.63}{\sqrt{1+K'}}, \quad \text{for longitudinal component,} \qquad (3)$$

$$\frac{0.92}{\sqrt{1+K'}}, \quad \text{for lateral component,} \qquad (4)$$

(Sathapornnanon et al., 1999). The last two equations are the modifications of the theoretical results of Dryden and Schubauer (1947) using the experimental results of Townsend (1951). For nomenclature in these equations, see Part II.

Secondly, to the question of the open-area ratio of the screens, as Bradshaw (1965) pointed out, the use of screens of open-area ratios less than 0.57 generally causes instability of the flow behind them owing to random coalescing of the emerging jets, ultimately resulting in spanwise variation in boundary layer thickness and surface shear stress. Therefore, it is recommended that the screens with open area ratios more than 0.57 be used.

Thirdly, to the question of the number of screens, the determining factors are the desired factors of reduction in mean velocity variation and turbulence level (Eqs. 1-4) – particularly those of the lateral components. In addition, owing to a relatively low throughflow speed in a settling chamber - particularly at high contraction ratio, the percentage of loss through screens in a settling chamber is rather small compared to those of the upstream components. Therefore, loss should not be a limiting factor.

Fourthly, to the question of the spacing between screens, because small-scale turbulence generated by the wire wakes behind a screen generally requires a distance of 500 wire diameters to decay, and because multiple screens are most effective for the reduction of turbulence when they are mounted far enough apart so that the wire wakes of one screen decay before the next screen is reached, it is therefore recommended that the screens be spaced at least 500 wire diameters apart (Bradshaw and Pankhurst, 1964).

Finally, it is interesting to note that the factors of reduction of turbulence given in Eqs. 3 and 4 are the approximates at a point behind the screen. Due to the decay of turbulence, further reduction is achieved as the flow evolves downstream. Experimental results of Townsend (1951) suggest that, for a screen with mesh 16 and wire diameter of 0.25 mm, further reduction of approximately 50% for both components is achieved at the distance of 600 wire diameters downstream.

3. Contraction

Similar to screens, contractions also help removing mean velocity variation as well as turbulence. Batchelor (1953) gave the theoretical treatment of an axisymmetric contraction with a contraction ratio c as: the factors of reduction of *percentage* mean velocity variation,

$$\mu = \frac{1}{c^2}, \quad \text{for longitudinal component,} \qquad (5)$$

$$\nu = \frac{1}{\sqrt{c}}, \quad \text{for lateral component,} \qquad (6)$$

and the factors of reduction of turbulence intensity,

$$\mu' = \frac{1}{2c^2}\sqrt{3\left(\ln(4c^3)-1\right)}, \text{ for longitudinal component} \qquad (7)$$

$$\nu' = \frac{1}{2}\sqrt{\frac{3}{c}}, \text{ for lateral component.} \qquad (8)$$

For nomenclature in these equations, see Part I.

Uberoi (1956) studied the effect of square contractions of area ratios 4, 9, and 16 on isotropic grid-generated turbulence by measuring turbulence velocity fluctuations at various points from inlet to exit. The results showed decrease in absolute magnitude for the longitudinal component and increase for the lateral component for the contraction ratios of 4 and 9. This is in agreement with the theoretical results in Eqs. 7 and 8. (Note that Eqs. 7 and 8 are the equations for the ratios of the relative turbulence intensity at the exit to that at the

inlet, not for the ratios of the absolute magnitudes of turbulence velocity fluctuation. To get the ratios of the absolute magnitudes of the turbulence velocity fluctuation, multiply the corresponding equation by the contraction ratio c. This also applies to Eqs. 5 and 6.) However, for the contraction of area ratio 16, the longitudinal component first decreased and then increased as the flow reached the contraction exit.

In addition, further measurements in the test section downstream of the contraction exit showed slight increase in the longitudinal component and decrease in the lateral component and, as a result, the turbulent energy in all three components tended to equalize. The results showed that the decrease in energy of the lateral component was due mainly to viscosity than to the transfer of energy to the longitudinal component, whose energy, as a result of this transfer, slightly increased.

It is interesting to note that there seems to be no general consensus regarding the best wall shapes for a contraction. Various wall shapes were studied and used, ranging from an eye-design, a polynomial, matched cubic arcs, matched elliptic arcs, etc. The choice, to some extent, depends primarily on the experience of the designer and the ease of making. The most common shapes, nonetheless, seem to be based on polynomials of various degrees. However, irrespective of wall shapes, for finite length contractions, there are regions of adverse velocity gradient on the walls at each end (Bradshaw and Pankhurst, 1964). In other words, the wall-velocity has a local minimum near an inlet and a local maximum near the exit. Hence, there are dangers in having flow separation at both ends. As a general guideline, it is desirable to have a relatively large radius of curvature at the inlet and a relatively small radius of curvature at the exit to avoid flow separation.

Other desirable properties required of a contraction besides the uniformity of the exit flow and the avoidance of having flow separation are minimum length and minimum exit boundary layer thickness. However, there is a trade off between the length and the boundary layer thickness. A short contraction runs the risk of having flow separation owing to too steep pressure gradient while a long contraction causes thick exit boundary layer. Generally, the suitable length of contraction ranges between 1 to 1.5 times the inlet diameter. For further details on the design of contractions, see, for example, Bradshaw and Pankhurst (1964), Morel (1975,1977), and Downie et al. (1984).

4. The settling chamber and the contraction of the FMRL blower tunnel

The settling chamber has a nominal inner cross-section of 100x100 cm^2 (102x102 cm^2 actual) and length of 134 cm. Flow conditioning devices in the settling chamber consist of (see Fig. 1 in Part I), from upstream to downstream, a screen of mesh 4 and wire diameter of 0.6 mm ($\beta = 0.82$, $K' = 0.27$); a honeycomb made of sections of PVC pipe, 15 mm in inner diameter, 1 mm thick, and 125 mm long (length-to-diameter ratio of 8.3 and approximately 60 cells per settling chamber width), sandwiched between two mesh 4 screens; and a series of seven household screens of mesh 16 and wire diameter of 0.24 mm ($\beta = 0.72$, $K' = 0.54$). The spacing between devices are uniform at approximately 130 mm.

Flow conditioning devices, i.e., honeycomb and screens, are constructed on wooden frames. The frames are 102x102 cm^2 in inner dimensions, 10 cm in width, and 4.3 cm in thickness. Each of the seven screens is sandwiched between a pair of frames. In the making, the screen is stretched and stapled onto one of the frame and the two frames are tightened together with bolts and nuts. Similarly, five frames are used for the honeycomb. The three inner frames support the staggered pipe sections, the two outer frames at each end sandwich the end screen, and the five frames are tightened together with bolts and nuts. There are total of 29 frames, 14 for the screens, 5 for the honeycomb, and the rests are used as spacer frames.

The structure of the settling chamber is made of wood, built into a box-like structure with flanges at both ends. The floor and the ceiling of the settling chamber are made of aluminum plates while the side walls are made of ply wood 15 mm thick. Both side walls can be easily removed. By designing the settling chamber as a box and frame inserts this way, the flow conditioning devices can be arranged and re-arranged as desired, and the screens can be easily removed for cleaning. The spacers can be used to adjust or change the spacing between screens as needed. In the current configuration, the spacing between screens is uniform at 130 mm, one spacer between screen-assemblies.

Owing to the difficulty in the making, for the contraction we made no attempt in doing any elaborate design calculation except taking some general guidelines into considerations. In addition, from our past experience the polynomial of degree 4 seems to work quite well (Rassame et al., 1998). Therefore, the shapes of both pairs of walls, top-bottom and left-right, are polynomials of the form

$$y(x) = a_o + a_1 x + a_2 x^2 + a_3 x^3 + a_4 x^4, \qquad (9)$$

which allows for five specified conditions. The five conditions that we choose are the positions and slopes of the wall at the inlet and the exit, and the location of the inflection point, i.e.,

at the inlet: $y(0) = \frac{W_1}{2}$, $y'(0) = 0$,

at the exit: $y(L) = \frac{W_2}{2}$, $y'(L) = 0$,

at the inflection: $y''(x_I) = 0$,

where W_1 and W_2 are the widths of the inlet and the exit respectively, L is the contraction length, x_I is the location of the inflection point, and the origin of the coordinates is at the center of the inlet. In the current configuration, the top and the bottom walls have the

profile, looking from side view, with W_1=100 cm, W_2=18 cm, L=1.5W_1=150 cm, and x_I^*=(2/3)L, and both side walls have the profile, looking from top view, with W_1=100 cm, W_2=60 cm, L=1.5W_1=150 cm, and x_I=(2/3)L. Figures 1a and 1b show the normalized profiles, $y^*(x^*)$, as well as the first and the second derivatives of the normalized profiles, $y^{*\prime}$ and $y^{*\prime\prime}$, of the top-bottom and the side walls respectively, where $x^* = x/L$ and $y^* = y/L$.

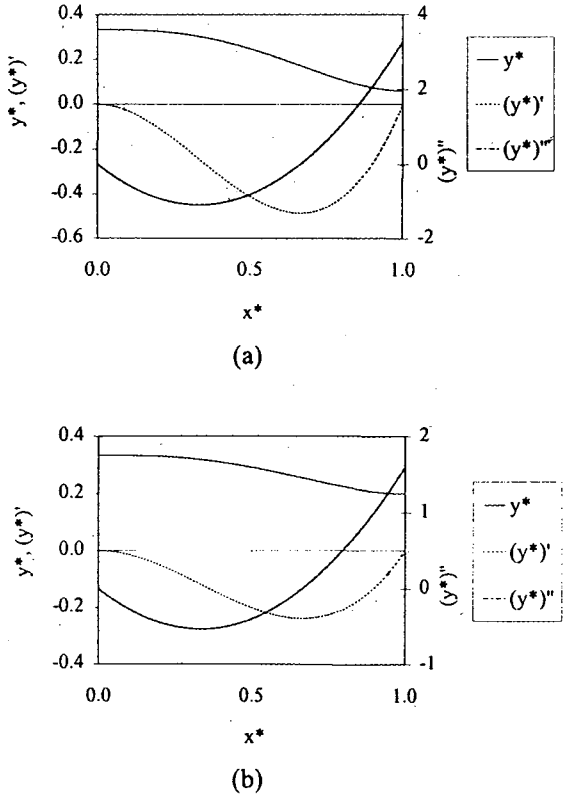

Fig. 1. Normalized contraction-wall shape and its first and second derivatives: (a) top and bottom walls, (b) side walls.

The total length is chosen to be 1.5 times the inlet width to avoid large pressure gradient (in the making, an additional straight section of 10 cm is added at each end for ease of support) and the inflection point is chosen to be located at (2/3)L to allow for a relatively large radius of curvature at the inlet. For comparison, if the inflection point is located at (1/2)L, we have an anti-symmetrical S-curve with a linear second derivative and with equal radii of curvature at the inlet and the exit. This is to be avoided, especially if the contraction length is short, for it runs the risk of having flow separation at the inlet owing to steep adverse pressure gradient.

The contraction is made of 2.5-mm thick steel plates. For the construction, the resulting wall profiles were first transformed into the actual plate profiles for cutting. Then, the plates were cut and rolled at the wide ends into the desired shapes. (The original plan was to roll at both ends. However, due to some mishaps, only the wide ends were rolled.) All four walls were then welded at the wide end first. Then, the plates were gradually heated, bent into shape, and welded at the narrow end. In this bending process, the bottom wall was slightly bent out of shape, resulting in a strip of locally high curvature along the span at approximately 33 cm upstream of the contraction exit flange. After finished, the shapes of all four walls were checked with templates and the local error of the profiles was found to be within $\pm$ 1.5 cm.

5. Calibration Schemes

Two types of calibration were conducted. For uniformity of the mean flow, the velocity distribution at the contraction exit was measured. For the boundary layer thickness, the boundary layer profile was measured. As mentioned in the Introduction, unfortunately, the turbulence intensity could not be measured at this time. Both types of calibration were done for two tunnel speeds, corresponding to the settings of an inverter of 25 Hz and 50 Hz. Only the results for 50 Hz setting are presented in details.

The measurements of the mean velocity distribution were done with a standard pitot probe with inner diameter of 1.5 mm and outer diameter of 4 mm. The measurements were made at the location approximately 0.5 cm upstream of the contraction exit flange, i.e., approximately 9.5 cm downstream of the zero-slope termination point. The spatial resolution of the measurement grids was 4 cm x 2 cm. The measurement grids, the coordinates system employed, and the designation for each wall as viewed from downstream of the contraction are shown in Fig. 2a.

The measurements of the boundary layer thickness were done by measuring the velocity distribution in the boundary layers along the periphery of the contraction exit. Since it was expected that the boundary layers were thin, a smaller probe than the existing standard probe was needed. Therefore, a smaller laboratory-built pitot probe was made. This probe was made from a hypodermic needle with inner diameter of 0.8 mm, outer diameter of 1.2 mm, and length of 11 cm. To make a pitot probe, the sharp end of the needle was cut straight and filed, to make a probe tip. Care was taken in filing so that the probe tip was circular – inside and outside - by carefully filing the cut mark off without bending the needle. (After removing the plastic receptor, the other end could be used as a tip too. Some filing may still be necessary.) Then, the stem was bent 90° at approximately 3 cm from the probe tip, resulting in the straight section from the tip to the stem approximately 27 mm – 22.5 times the outer diameter of the probe. The plastic receptor at the other end of the needle was then removed, and the needle was inserted and glued into a stainless steel tube of inner diameter 2 mm, outer diameter 5 mm, and length 32 cm. The length of the straight section of the needle between the bent and the stainless steel tube was approximately 5 cm. The probe was then calibrated against the standard

probe employed in the measurement of the mean velocity distribution over the range of 2 to 15 m/s, no significant deviation was detected.

The measurements of the boundary layer profile were done at a total of 16 locations along the periphery of the contraction exit – at 5 and 3 uniformly-spaced locations along each wider and each narrower wall, respectively - and at the same streamwise location as the measurements of the mean velocity distribution. Figure 2b shows the measurement locations. For the measurements, the probe was traversed at 1-mm step from the wall. On the one hand, since the boundary layers were relatively thin compared with the size of the probe, but on the other hand, since only the thicknesses, not the profiles, were desired, no elaborated correction scheme was applied to the measurement data to correct for the effects of the probe size, of wall proximity, etc.

Finally, all the pressure measurements were made with an Auto Tran Inc. pressure transducer model 750D-212 with range ± 0.5" WG and accuracy (supplied by the manufacturer) 0.25% FS.

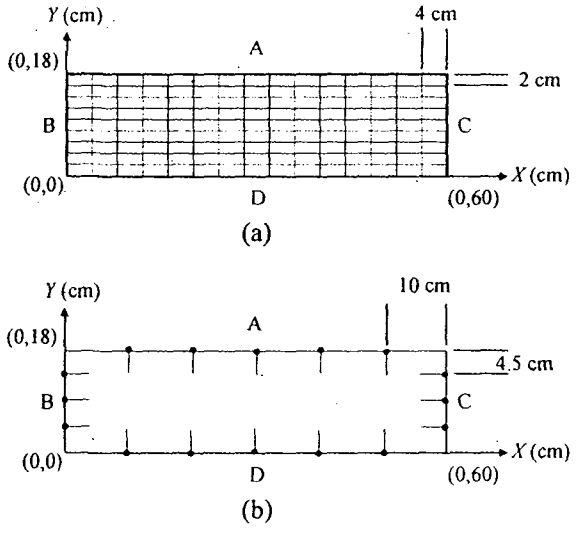

Fig. 2. Coordinates system and measurement grids: (a) for mean velocity, (b) for boundary layer profile.

6. Results and discussion

Figure 3a shows the mean velocity distribution at the contraction exit for an inverter setting of 50 Hz. The uncertainty in the measurement is estimated to be ± 0.08 m/s. For the contour plot, the velocities at the grid points on each wall are substituted with the average value of the freestream velocities from the boundary layer measurements along that wall. The average velocity over the cross section is then determined to be 13.95 m/s with the non-uniformity of ± 0.2 m/s, a non-uniformity of less than ± 1.5%.

Similarly, for an inverter setting of 25 Hz (Fig. 3b), the average velocity is determined to be 7.29 m/s with the non-uniformity of ± 0.07 m/s. However, the uncertainty for the measurements in this case is estimated to be ± 0.16 m/s. Therefore, the non-uniformity is estimated to be less than ± 2.2%.

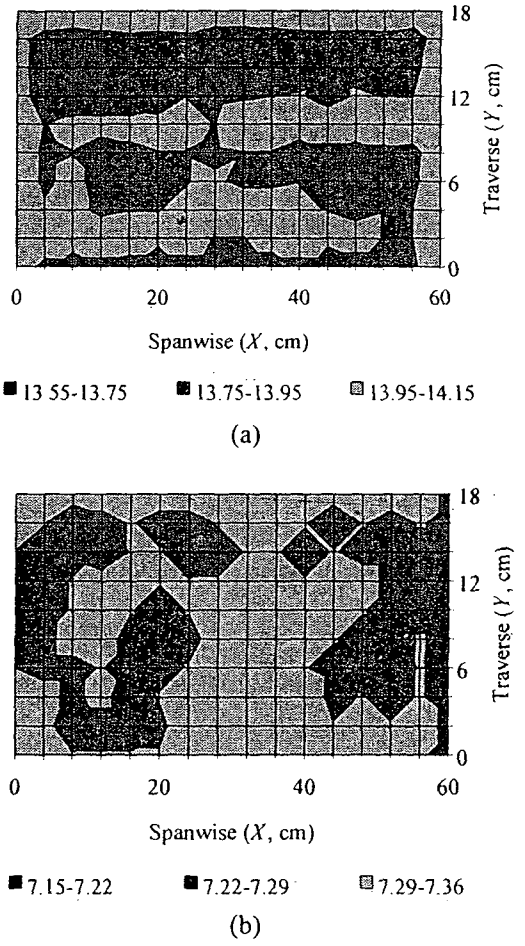

Fig. 3. Mean velocity distribution at the contraction exit: (a) inverter setting 50 Hz, (b) inverter setting 25 Hz.

The results for boundary layer measurement for the case of an inverter setting of 50 Hz are shown in Figs. 4a to 4d. The average boundary layer thicknesses along walls A, B, C, and D are determined to be less than 3, 3, 3, and 4 mm, respectively, the overall average of less than 3 mm. The results show that the thickness of the boundary layer along each wall is relatively uniform. Nonetheless, some irregularity seems to be present along wall D (the bottom wall). Since the spatial resolution of the measurements is relatively low, we offer no further details regarding the boundary layer profiles. It suffices to mention, however, that such irregularity, if it exists, will not cause any difficulty in our planned research programs. The reason is that, in our programs, thick turbulent boundary layers are required.

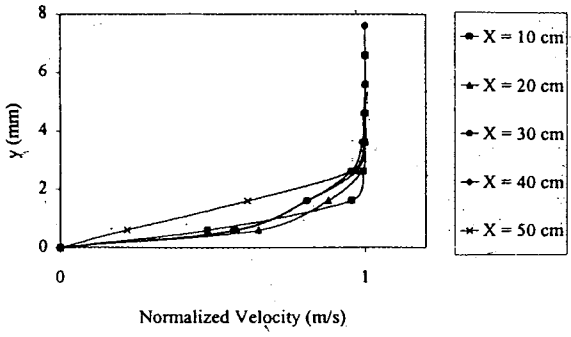

(a)

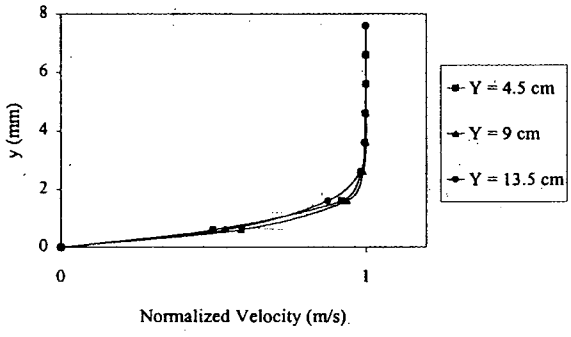

(b)

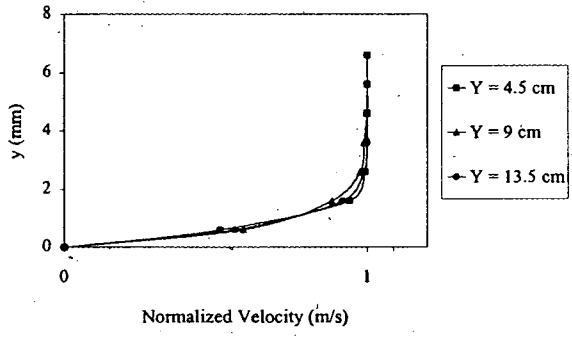

(c)

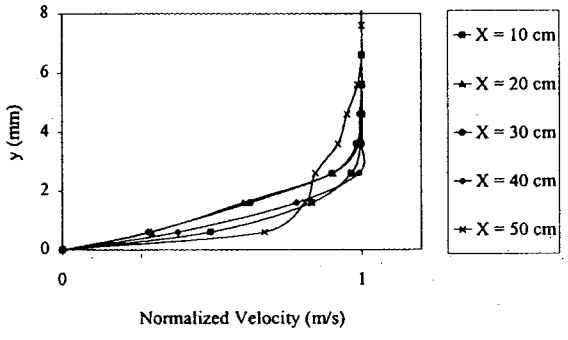

(d)

Fig. 4. Normalized boundary layer profiles along the contraction exit walls : (a) wall A, (b) wall B, (c) wall C, (d) wall D.

For the case of an inverter setting of 25 Hz, the average boundary layer thicknesses along walls A, B, C, and D are less than 4, 3, 3, and 6 mm, respectively, the overall average of less than 4 mm.

7. Conclusions

This is the last part in the series of three papers describing the design and development of the Fluid Mechanics Research Laboratory (FMRL) 60x18 cm^2 wide-angle screened-diffuser blower tunnel. In this part, the design and development of the settling chamber and the contraction were discussed. The calibration schemes for the quality of the flow generated as well as the results were reported.

For the current configuration, the maximum speed of the tunnel, measured at the contraction exit, was determined to be 13.95 m/s with the non-uniformity of $\pm$ 0.2 m/s, a non-uniformity of less than $\pm$ 1.5%. The average boundary layer thickness over the periphery of the contraction exit was less than 3 mm. At another lower speed, the speed of 7.29 m/s, the non-uniformity was estimated to be less than $\pm$ 2.2%, and the average boundary layer thickness was less than 4 mm.

From the calibration results, we conclude that the tunnel performs quite satisfactorily. The quality of the flow generated is more than sufficient and well suite for our planned research programs.

References

1. Batchelor, G. K., (1953), The theory of homogeneous turbulence, Cambridge University Press, Cambridge.
2. Bradshaw, P., and Pankhurst, R. C., (1964), "The design of low-speed wind tunnels," *Prog. Aero. Sci.*, Vol. 5, pp. 1-69.
3. Bradshaw, P., (1965)," The effect of wind-tunnel screens on nominally two-dimensional boundary layer," *J. Fluid Mech.*, Vol. 22, pp. 679-687.
4. Downie, J. H., Jordinson, R., and Barnes, F. H., (1984), "On the design of three-dimensional wind tunnel contractions," *Aero. J.*, September, 1984, pp. 287-295.
5. Dryden, H. L., and Schubauer, G. B., (1947), "Use of damping screens for reduction of wind tunnel turbulence," *J. Aero. Sci.*, Vol. 14, p. 221.
6. Loehrke, R. I., and Nagib, H. M., (1976), "Control of free-stream turbulence by means of honeycombs: A balance between suppression and generation," J. Fluids Engineering, September, 1976, pp. 342-353.
7. Morel, T., (1975), "Comprehensive design of axisymmetric wind tunnel contractions," *J. Fluids Engineering*, June, 1975, pp. 225-233.
8. Morel, T., (1977), "Design of two-dimensional wind tunnel contractions," *J. Fluids Engineering*, June, 1977, pp. 371-378.
9. Rassame, S., Siripoorikan, B., Buensawang, S., Petitanalap, Y., and Bunyajitradulya, A., (1998), "Visualization of fluid flows using the smoke-wire technique," *Research and Development Journal of The Engineering Institute of Thailand*, Vol. 9, No. 2, pp. 71-87.

10. Sathapornnanon, S., Wattanawanichakorn, A., Trakulmaipol, S., Lumluksana-paiboon, M., Pimpin, A., and Bunyajitradulya, A., (1999), "The Design and Development of The FMRL 60x18 cm^2 Wide-Angle Screened-Diffuser Blower Tunnel, Part II: The Screened Diffuser," Proceeding of the 13th National Mechanical Engineering Conference, 2-3 December 1999, Royal Cliff Beach Resort Hotel, South Pattaya, Cholburi.
11. Townsend, A. A., (1951), "The passage of turbulence through wire gauzes," *Quart. J. Mech. Appl. Math.*, Vol. 4, p. 308.
12. Uberoi, M. S., (1956), "Effect of wind-tunnel contraction on free-stream turbulence," *J. Aero. Sci.*, August, 1956, pp. 754-764.